Proceedings of the 21st ICSMGE, Vienna, Austria, 14 – 19 June 2026. Pistrol, Adam & Schweiger (eds.)
Published by: ÖGG, Austrian Society for Geomechanics, Salzburg, Austria, ISBN 978-3-9503898-4-5
https://doi.org/10.53243/ICSMGE2026-571

Mechanical Characterization of DSM Materials for Structural Use

Marissabelle Mrad, Olivier Cuisinier, Farimah Masrouri
Université de Lorraine, CNRS, LEMTA, F-54000 Nancy, France

ABSTRACT: Deep Soil Mixing (DSM), developed in the 1960s in Japan and the Nordic countries, improves in-situ soil properties by mixing them with hydraulic binders. While traditionally used for ground improvement applications such as embankment stabilization, liquefaction mitigation, and cut-off walls, DSM is increasingly being adopted for temporary and permanent retaining structures due to its lower environmental impact and cost-effectiveness. However, the mechanical behavior of DSM materials, particularly under conditions relevant to retaining structures, remains insufficiently understood. This study evaluates the mechanical behavior of DSM materials prepared with natural silt from northeastern Paris (LP) and a laboratory-reconstituted soil by blending the silt with Moselle sand (LPMS), using a slag-based cement (CEM III/C 32.5 N) at dosages of 150, 250, and 400 kg/m³. Specimens were cured at 40 °C for 56 days and tested under unconfined compression and low-level cyclic loading. Unconfined compressive strength (UCS) results revealed a substantial increase between 150 and 250 kg/m³ cement content (from 5.3 to 10.7 MPa), followed by a plateau at 400 kg/m³. For the same cement dosage, the LPMS mixture showed a 1.5-fold increase in UCS compared to LP 150, attributed to lower porosity and denser packing. Cyclic loading tests revealed a transition in mechanical behavior: LP 150 exhibited a ductile, soil-like response with significant strain accumulation, while LP 400 and LPMS 150 showed stiff, quasi-elastic behavior with minimal hysteresis and near-overlapping cycles. Despite similar UCS values, LP 250 and LP 400 exhibited distinct cyclic responses, highlighting that UCS alone is insufficient for characterizing DSM behavior. The findings underline the critical influence of both cement dosage and soil composition on stiffness and deformation response. The term “soilcrete” thus oversimplifies the diversity of DSM products. Identifying mixtures that exhibit stable elastic behavior at service stress levels is essential for design reliability.

KEYWORDS: Deep Soil Mixing, Retaining Structures, Soilcrete, Mechanical Behavior.

1 INTRODUCTION

In response to increasing environmental concerns, the use of construction techniques with lower ecological impact is on the rise. In geotechnical engineering, Deep Soil Mixing (DSM) has emerged as a sustainable method that improves in situ soil by mechanically mixing it with hydraulic binders. By avoiding soil extraction and reducing transportation needs, DSM helps minimize CO_2 emissions. Soil improvement results from mechanisms such as ion exchange on clay surfaces, particle bonding, and void filling with cementitious products (Terashi, 2003). DSM has been widely adopted over the past five decades for applications including foundation support, embankment stabilization, cut-off walls, and site remediation. More recently, it has gained interest for use in retaining structures, offering advantages over traditional methods (e.g., soldier piles, diaphragm walls) due to its adaptability, lower noise and vibration, and cost-efficiency (Rutherford, 2005). However, the extension of DSM from conventional ground improvement to structural applications introduces new performance requirements. These include enhanced strength and stiffness, effective deformation control, and long-term durability under sustained and cyclic loading conditions.

The DSM process produces a heterogeneous, multiphase composite material commonly referred to as “soilcrete”. However, this term remains questionable in both practice and literature, as the transition from improved soil behavior to concrete-like behavior is not well-defined. Reported compressive strengths vary widely. According to Bruce (2000), values range from 0.2–2 MPa for cohesive soils and 0.5–5 MPa for granular soils, depending on cement content. In contrast, other studies (Ganne et al., 2011; Szymkiewicz, 2011; Helson, 2017) report strengths reaching 7–30 MPa for clayey and sandy soils, respectively.

For retaining structures, this wide range of material strength and behavior is critical: performance requirements such as load-bearing capacity, bending stiffness and soil–structure interaction must be reliably met to ensure safety, serviceability, and durability. The hydro-mechanical behavior of DSM material is influenced by numerous factors, including native soil type, binder composition and dosage, mixing technique, and curing conditions (Terashi, 1997; Porbaha, 2002; Bruce et al., 2013). These result in a material whose behavior ranges from ductile and soil-like to rigid and concrete-like, making the prediction and standardization of DSM mechanical response particularly challenging when used in structural applications.

Consequently, the design and analysis of DSM walls remain largely empirical and based on simplified assumptions, due to limited understanding of their complex behavior across different soils (Abas, Alluqmani and Yousif, 2023). In the literature, a range of constitutive models have been used in finite element modeling to represent DSM behavior. The Mohr-Coulomb model is widely adopted due to its simplicity (Cuira et al., 2013; Grzyb-Faddoul, 2014), while more advanced models such as the Hardening Soil Model (Cuira et al., 2013), and Concrete Damage Plasticity Model (Larsson et al., 2012) have also been employed. Nevertheless, no consensus exists regarding the appropriate constitutive law for DSM materials, and the conditions under which each model should be applied remain poorly defined.

In this context, the present study seeks to identify the mechanical behavior threshold at which DSM material begins to behave like concrete, and thus could be justifiably referred to as "soilcrete". This work builds on the insights of Denies and Huybrechts (2018) and Bruce et al. (2013), who highlight that the use of DSM for structural applications, such as retaining structures, is feasible primarily in sandy and silty soils, provided the mixtures exhibit high homogeneity and relatively high binder content is used. In line with these criteria, this study investigates laboratory-prepared specimens composed of silty soil combined with three different cement dosages, selected to reflect the range of binder contents typically encountered in practical DSM implementations. Cyclic loading tests were employed to assess mechanical behavior. Unlike conventional cyclic tests typically used to evaluate fatigue or dynamic properties, this study applies a low number of cycles (3), which offers valuable insights into material behavior, such as loading history effects, strain nonlinearity, deformation accumulations, and hardening responses.

2 MATERIALS AND METHODS

2.1 *Materials*

The selected soil is "Limon des plateaux" collected from the northeastern part of Paris, and a sandy soil from the Moselle, "Sable de Moselle". The soil's basic properties are shown in Table 1.

Table 1. Basic properties of the studied soil.

Soil	Properties	Value
Limon des plateaux (LP)	Liquid limit (%)	36.8
	Plastic limit (%)	22.5
	Plasticity index (%)	14.3
	Soil particles density (Mg/m^3)	2.65
	Particles < 63 µm (%)	95
	VBS	2.8
Sable de Moselle (MS)	Maximum void ratio	0.69
	Minimum void ratio	0.52
	Uniformity coefficient, Cu	5.88
	Curvature coefficient, Cc	1.24
	Maximum grain diameter (mm)	2
	Soil particles density (Mg/m^3)	2.64

The cement used in this study is a slag-based binder, CEM III/C 32.5 N - SR CE PM NF, provided by ROMBAS Heidelberg Materials. This cement contains 15% clinker, with a mineralogical composition of 68% C_3S, 10% C_2S, 9.8% C_3A, and 8.9% C_4AF. The remaining 85% consists of ground granulated blast furnace slag (GGBFS), primarily vitreous (99%). The chemical composition of the slag is characterized by a $(CaO + MgO)/SiO_2$ ratio of 1.3, with CaO, MgO, and SiO_2 collectively accounting for 85% of its total mass. According to the NF EN 196-1 standard (AFNOR, 2016), compressive strength tests indicate that by day 7, the cement achieves 95% of the normalized strength reported in the product technical data sheet.

2.2 *Mix proportions and specimen preparation*

The "LP" soil was mixed with three cement dosages 150, 250, and 400 kg/m^3, based on the total volume of the mixture. Additionally, a laboratory-reconstituted soil, composed of 50% LP and 50% MS (denoted as "LPMS"), was prepared and treated with 150 kg/m^3 of cement. These dosages were selected based on criteria outlined in (Denies and Huybrechts, 2018) (Bruce et al., 2013), which indicate that the feasibility of DSM for retaining structures requires a homogeneous material, the exclusion of clayey soils, and the use of relatively high cement contents.

After fixing the cement dosages, a parametric study was conducted to determine the optimal total water content for each mixture. The objective was to ensure high workability comparable to that observed in in-situ DSM applications while avoiding material bleeding, which could compromise laboratory results. Based on this, a total water content (w_{Tot}) of 48% was identified for all three LP-based mixtures, and 32% for the LPMS mixture, corresponding to a target slump flow of 25 ± 2 cm. These values satisfy both the workability and anti-bleeding criteria.

The preparation method consisted of hand-mixing the soil and cement until visually homogeneous, followed by the addition of water into the mixer and blending at a rotation speed of 60 rpm for 10 minutes to ensure a homogeneous and repeatable material. The fresh material was placed into cylindrical molds (100 × 50 mm) in three layers, with each layer compacted by tapping. The specimens were then cured at 40 °C for 56 days before testing. The curing protocol was selected based on a preliminary study that established its equivalence to approximately 180 days of curing at 20 °C. The use of higher temperature was intended to accelerate strength development and reduce the overall curing period, while maintaining the mechanical representativeness of the material (Escalante-García and Sharp, 1998).

2.3 *After curing specimen characteristics*

The water-accessible porosity (n) and dry density (ρ_d) of each mixture were measured after 56 days of curing at 40 °C. The results are summarized in Table 2.

Table 2. Physical characteristics of specimens after 56 days of curing at 40°C.

Mix design ID	n (%)	ρd (Mg/m^3)
LP 150	53 ± 0.9	1.21
LP 250	42 ± 0.8	1.33
LP 400	40 ± 1.2	1.37
LPMS 150	39.5 ± 0.08	1.51

2.4 *Mechanical tests*

2.4.1 *Unconfined compression testing*

Unconfined compressive strength (UCS) tests were performed on soil–cement mixture specimens after 56 days of curing using a universal testing machine with a maximum capacity of 50 kN. The experimental procedure adhered to the EN 13286-41 standard (Test method for the determination of the compressive strength of hydraulically bound mixtures), applying a constant vertical displacement rate of 1.0 mm/min. This testing rate was selected to ensure that specimen failure occurred within 30 to 120 seconds from the onset of loading, as prescribed by the standard.

UCS was determined by dividing the peak axial load by the initial cross-sectional area of the specimen. For each mixture type, three specimens were tested to ensure repeatability, and the average UCS value was calculated and reported.

2.4.2 *Stress-strain behavior testing*

The stress–strain behavior of the mixtures was evaluated using a test setup equipped with two local vertical displacement transducers for axial strain measurement. The use of dual transducers and averaging of their readings minimized potential errors due to specimen bending during testing. Radial strains were monitored using a circumferential chain extensometer. The complete experimental setup is illustrated in Figure 1.

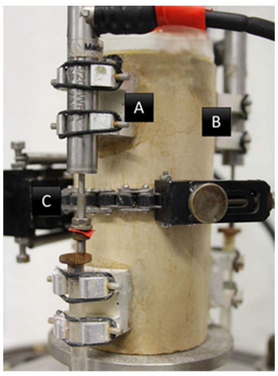

Figure 1. Experimental set-up: A, B – axial displacement transducers; C– circumferential chain.

The loading protocol followed the NF EN 12390-13 standard and was applied to two specimens per mixture. The procedure began with three conditioning cycles between a preload stress $\sigma_p = 0.5$ MPa and a lower stress limit equivalent to σ_b=20% of the UCS, to verify the stability of the instrumentation and the proper alignment of the specimen. Subsequently, cyclic loading was applied between the lower stress level σ_b and an upper stress level σ_a equal to 30% of the UCS by maintaining each stress level for a period less than 20 seconds to characterize the response of the material under repeated loading. The modulus was then measured during the loading cycles, the initial secant modulus obtained from the first cycle, and the stabilized modulus from the third cycle.

3 RESULTS AND DISCUSSION

The UCS values obtained from laboratory testing are presented in Table 3. The UCS of the soil–cement mixtures are strongly influenced by the material's microstructure, particularly porosity and the formation of cementitious bonds between soil particles. A notable increase in UCS is observed between mixtures LP 150 and LP 250, which corresponds to a significant reduction in porosity. This improvement is primarily attributed to enhanced cementitious bonding and the filler effect of the cement particles. However, the increase in UCS between LP 250 and LP 400 is marginal, indicating the presence of a cement content threshold beyond which additional cement has a limited impact on strength development. This plateau effect may result from the saturation of binding sites or the limited contribution of excess cement to additional bonding once a critical mixture density has been achieved. Notably, at the same cement dosage of 150 kg/m³, the LPMS 150 mixture exhibits a UCS approximately 1.5 times higher than that of LP 150. This is primarily attributed to the lower water content required to achieve comparable workability, which leads to a reduced post-curing void ratio and a denser microstructure.

Table 3. UCS results after 56 days of curing at 40˚C.

Mix design ID	UCS (MPa)
LP 150	5.3 ± 0.3
LP 250	10.7 ± 0.1
LP 400	10.8 ± 0.1
LPMS 150	8.10 ± 0.03

The results of the secant modulus determination for all prepared mixtures are presented in Table 4. The stress–axial strain responses of the LP mixtures are shown in Figure 2. For the LP 150 specimens, the strain amplitude decreases progressively from cycle 1 to cycle 3. The first loading cycle exhibits a pronounced non-linear stress–strain response, indicative of a stiffening effect. This behavior is likely due to pore collapse, structural rearrangement, or compaction of the soil matrix during the initial loading. Consequently, the secant modulus increases with each successive cycle. The near-superposition of cycles 2 and 3 suggests that the material reaches a stabilized mechanical response after the first cycle. The LP 250 specimens exhibit a similar trend but with less pronounced non-linearity during the first cycle, indicating a stiffer initial structure compared to LP 150. In contrast, the LP 400 specimens display an almost linear and repeatable stress–strain response across all three cycles. The overlapping of the curves reflects a more rigid and stable internal structure, less susceptible to rearrangement under cyclic loading. These findings underscore the influence of cement dosage in governing the mechanical response of DSM materials, which ranges from soil-like behavior (LP 150) to concrete-like behavior (LP 400).

Further evidence is provided in Figure 3, where axial, radial, and volumetric strains are plotted separately for LP 150 and LP 400. LP 150 exhibits marked radial expansion during the first cycle and accumulates permanent deformation, whereas LP 400 shows negligible radial strain, confirming its elastic stability under identical stress levels.

Furthermore, Figure 4 compares the stress–axial strain curves for mixtures with identical cement dosage (150 kg/m³) but different soil types: LP 150 and LPMS 150. The results demonstrate the substantial influence of soil composition on mechanical behavior. The LPMS 150 mixture exhibits a quasi-elastic response, which is primarily attributed to its higher density, lower porosity, and the presence of coarser granular particles. This highlights the important role of aggregate type, a known factor influencing stiffness and modulus in cementitious materials, even in conventional concrete.

Table 4. Initial and stabilized secant modulus of all mixtures

Mix design ID	$E_{c,0}$ (MPa)	$E_{c,s}$ (MPa)
LP 150	787	3135
LP 250	2986	6095
LP 400	6568	6956
LPMS 150	6392	7606

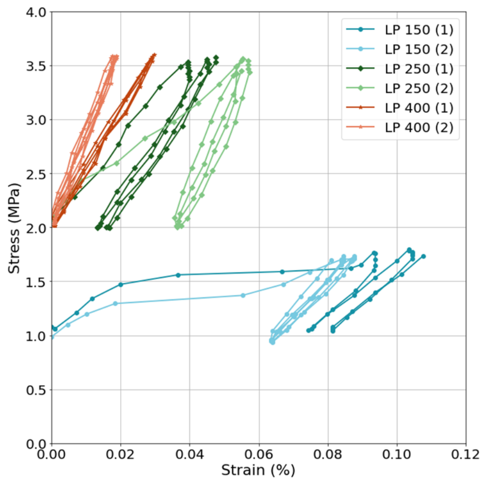

Figure 2. Stress-axial strain diagrams during cyclic loading between 20% UCS and 30% UCS.

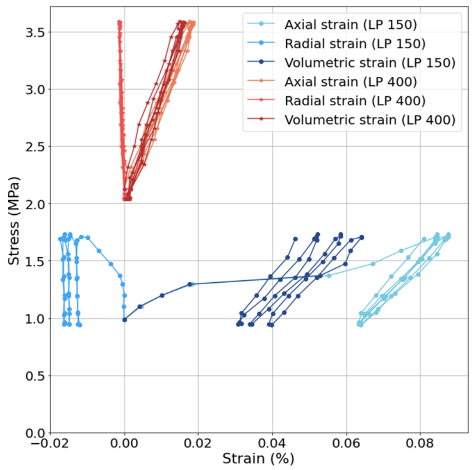

Figure 3. Stress-strain diagrams with components of the strains: axial, radial, and volumetric strain.

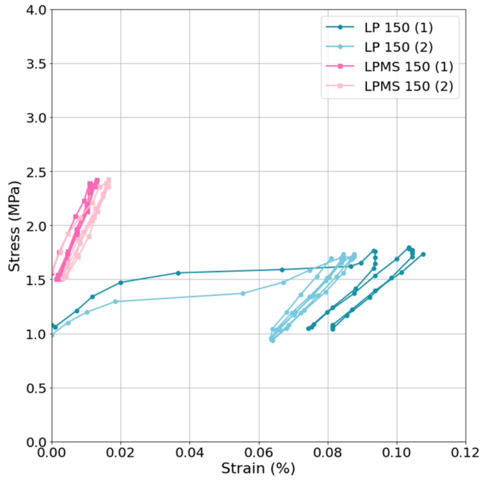

Figure 4. Stress-axial strain diagrams during cyclic loading between 20% UCS and 30% UCS.

4 CONCLUSIONS AND PERSPECTIVES

By systematically varying the two primary parameters in DSM, cement content and soil type (or more broadly, the fines content) while maintaining consistent workability and preparation methods, this study revealed a wide spectrum of mechanical behaviors in DSM materials. These ranged from ductile, soil-like responses at lower binder dosages (LP 150) to stiff, quasi-elastic behavior at higher dosages (LP 400). Notably, for a constant cement dosage of 150 kg/m³, the incorporation of 50% sand into the initial soil (LPMS 150) significantly altered the mechanical response, shifting it from a soil-like to a concrete-like behavior in terms of stress–strain non-linearity.

These findings underscore the diversity of DSM material behavior. Despite comparable UCS values between LP 250 and LP 400, cyclic loading tests revealed significant differences in their mechanical responses. LP 400 exhibited a stiffer, more linear stress–strain response with nearly overlapping cycles, indicative of elastic behavior and structural stability. In contrast, LP 250 showed earlier yielding and reduced stiffness, highlighting that UCS alone is insufficient to characterize the mechanical performance of DSM materials. The transition from soil-like behavior (LP 150) to concrete-like behavior (LPMS 150), even at the same cement dosage, further demonstrates the critical role of aggregate type and gradation. Moreover, differences in axial, radial, and volumetric strain evolutions emphasize the need to evaluate stiffness when assessing the performance of DSM mixtures for structural use.

In summary, identifying DSM formulations that exhibit stable, quasi-elastic behavior under service stress levels is essential for their deployment in permanent retaining structures, where deformation control, stiffness, and long-term durability are paramount.

After identifying DSM materials exhibiting concrete-like mechanical behavior, it becomes imperative to extend the investigation beyond short-term performance and evaluate their long-term durability. In permanent applications such as retaining structures, these materials are subjected to sustained mechanical loads and environmental solicitations, either through direct exposure of the excavated face or as a result of fluctuating groundwater levels affecting the embedded portion. Understanding the response of soil–cement mixtures to combined environmental and mechanical actions is therefore critical.

Future research will focus on evaluating the durability of DSM materials, particularly their behavior under wetting–drying cycles and sustained loading conditions. These studies aim to develop a comprehensive understanding of the long-term performance of DSM composites and to contribute to the establishment of robust design criteria for their structural application in geotechnical engineering.

5 ACKNOWLEDGEMENTS

The authors are grateful for the support of Fayat Fondations, particularly Hovhanessian Gilles, Puffeney Jean-Philippe, Fancelli Fabien, ESLAMI Hossein, and Michaud Emilien.

6 REFERENCES

Abas, Hassan.A., Alluqmani, A.E. and Yousif, I., 2023. Assessing deep soil mixing for excavation support in Sabkha soils: a numerical study. *Journal of Umm Al-Qura University for Engineering and Architecture*. [online] https://doi.org/10.1007/s43995-023-00036-y.

Bruce, D.A., 2000. *An Introduction to the Deep Soil Mixing Methods as Used in Geotechnical Applications*. Available at: <https://rosap.ntl.bts.gov/view/dot/40947>.

Bruce, M.E.C., Turner-Fairbank Highway Research Center, Geotechnica, S., Inc, and United States Federal Highway Administration Office of Transportation Management, 2013. *Federal Highway Administration design manual : deep mixing for embankment and foundation support*. [online] McLean, VA: U.S. Department of Transportation, Federal Highway Administration, Research, Development, and Technology, Turner-Fairbank Highway Research Center. Available at: <https://purl.fdlp.gov/GPO/gpo41642>.

Cuira, F., D'Aguiar, S., Grzyb, A., Pellet, F., Mosser, J.-F., Guimond-Barrett, A. and Le Kouby, A., 2013. Modélisation numérique du comportement d'une colonne de soil-mixing et confrontation à un essai de chargement en vraie grandeur. In: *18 th International Conference on Soil Mechanics and Geotechnical Engineering*. Paris.

Denies, N. and Huybrechts, N., 2018. *Handbook - Soil mix walls: Design and execution*. 1st ed.

Escalante-García, J.I. and Sharp, J.H., 1998. Effect of temperature on the hydration of the main clinker phases in portland cements: part i, neat cements. *Cement and Concrete Research*, 28(9), pp.1245–1257. https://doi.org/10.1016/S0008-8846(98)00115-X.

Ganne, P., Denies, N., Huybrechts, N., Vervoort, A., Tavallali, A., Maertens, J., Lameire, B. and De Cock, F., 2011. Soil mix: influence of soil inclusions on structural behaviour. Proceedings of the 15th European Conference on Soil Mechanics and Geotechnical Engineering. IOS Press. pp.977–982.

Grzyb-Faddoul, A.M., 2014. *Numerical analysis of the reinforcement of existing foundations by the soil mixing technique*. Doctoral thesis. INSA de Lyon.

Helson, O., 2017. *Comportement thermo-hydro-mécanique et durabilité des bétons de sol : influence des paramètres de formulation et conditions d'exposition.* [Doctoral thesis] UNIVERSITE DE CERGY-PONTOISE. Available at: <http://www.theses.fr/2017CERG0860/document>.

Larsson, S., Malm, R., Charbit, B. and Ansell, A., 2012. Finite element modelling of laterally loaded lime–cement columns using a damage plasticity model. *Computers and Geotechnics*, 44, pp.48–57.

Porbaha, A., 2002. State of the art in quality assessment of deep mixing technology. *Proceedings of the Institution of Civil Engineers - Ground Improvement*, 6(3), pp.95–120. https://doi.org/10.1680/grim.2002.6.3.95.

Rutherford, C.J., 2005. *Design manual for excavation support using deep mixing technology*. Doctoral thesis. Texas A&M University.

Szymkiewicz, F., 2011. *Évaluation des propriétés mécaniques d'un sol traité au ciment.*

Terashi, M., 1997. Theme lecture: Deep mixing method - Brief state of the art. In: *the International Society for Soil Mechanics and Geotechnical Engineering (ISSMGE)*, 14th ICSMFE. Hamburg. pp.2475–2478.

Terashi, M., 2003. The state of practice in deep mixing methods. In: *Grouting and ground treatment*. pp.25–49.